

AD-A236 759



AEOSR-TR- 91 0506

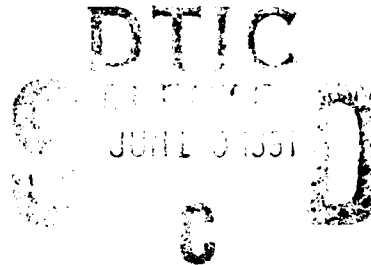
2

Annual Technical Report

on

**TURBULENT REACTING FLOWS
AND SUPERSONIC COMBUSTION**

Grant AFOSR-90-0151



Prepared for

AIR FORCE OFFICE OF SCIENTIFIC RESEARCH

For the Period

15 February 1990 to 14 February 1991

Submitted by

**C. T. Bowman
R. K. Hanson
M. G. Mungal
W. C. Reynolds**

Accession For	
DTIC GRAFI	<input checked="" type="checkbox"/>
DTIC TAB	<input type="checkbox"/>
Unannounced	<input type="checkbox"/>
Justification	
by	
Distribution/	
Availability Codes	
Avail and/or	
Dist	Special
A-1	



DISTRIBUTION STATEMENT A

Approved for public release;
Distribution Unlimited

**HIGH TEMPERATURE GASDYNAMICS LABORATORY
Mechanical Engineering Department
Stanford University**

91 6 6 018

91-01462



REPORT DOCUMENTATION PAGE

Form Approved
OMB No. 0704-0188

1a. REPORT SECURITY CLASSIFICATION Unclassified			1b. RESTRICTIVE MARKINGS	
2a. SECURITY CLASSIFICATION AUTHORITY			3. DISTRIBUTION / AVAILABILITY OF REPORT Approved for public release; distribution is unlimited.	
2b. DECLASSIFICATION / DOWNGRADING SCHEDULE				
4. PERFORMING ORGANIZATION REPORT NUMBER(S)			5. MONITORING ORGANIZATION REPORT NUMBER(S)	
6a. NAME OF PERFORMING ORGANIZATION Stanford University		6b. OFFICE SYMBOL (If applicable)	7a. NAME OF MONITORING ORGANIZATION AFOSR/NA	
6c. ADDRESS (City, State, and ZIP Code) Department of Mechanical Engineering Stanford, CA 94305			7b. ADDRESS (City, State, and ZIP Code) Building 410, Bolling AFB DC 20332-6448	
8a. NAME OF FUNDING / SPONSORING ORGANIZATION AFOSR/NA		8b. OFFICE SYMBOL (If applicable) NA	9. PROCUREMENT INSTRUMENT IDENTIFICATION NUMBER AFOSR-90-0151	
8c. ADDRESS (City, State, and ZIP Code) Building 410, Bolling AFB DC 20332-6448			10. SOURCE OF FUNDING NUMBERS	
			PROGRAM ELEMENT NO. 61103D	TASK NO. A1
			PROJECT NO. 3484	WORK UNIT ACCESSION NO.
11. TITLE (Include Security Classification) (U) Turbulent Reacting Flows and Supersonic Combustion				
12. PERSONAL AUTHOR(S) C. T. Bowman, R. K. Hanson, M. G. Mungal and W. C. Reynolds				
13a. TYPE OF REPORT Annual Technical Report		13b. TIME COVERED FROM 15-2-90 to 14-2-91		14. DATE OF REPORT (Year, Month, Day) 1991, March 15
15. PAGE COUNT 26				
16. SUPPLEMENTARY NOTATION				
17. COSATI CODES			18. SUBJECT TERMS (Continue on reverse if necessary and identify by block number)	
FIELD	GROUP	SUB-GROUP		
			turbulent reacting flow, supersonic combustion	
19. ABSTRACT (Continue on reverse if necessary and identify by block number)				
<p>An experimental and computational investigation of supersonic non-reacting and combustion flows is in progress. The principal objective of the research is to gain a more fundamental understanding of mixing and chemical reaction in supersonic flows. The research effort comprises three inter-related elements: (1) an experimental study of mixing and combustion in a supersonic plane mixing layer; (2) development of laser-induced fluorescence techniques for time-resolved two-dimensional imaging of species concentration, temperature, velocity and pressure; and, (3) numerical simulations of compressible reacting flows. The specific objectives and the status of the research of each of these program elements are summarized in this report.</p>				
20. DISTRIBUTION / AVAILABILITY OF ABSTRACT <input checked="" type="checkbox"/> UNCLASSIFIED/UNLIMITED <input checked="" type="checkbox"/> SAME AS RPT. <input checked="" type="checkbox"/> DTIC USERS			21. ABSTRACT SECURITY CLASSIFICATION Unclassified	
22a. NAME OF RESPONSIBLE INDIVIDUAL Julian M Tishkoff			22b. TELEPHONE (Include Area Code) (202) 767-4935	22c. OFFICE SYMBOL AFOSR/NA

TABLE OF CONTENTS

	Page
1.0 SUMMARY	1
2.0 INTRODUCTION	2
3.0 MIXING AND REACTION IN SUPERSONIC FLOW	3
3.1 Objectives.	3
3.2 Status of the Research.	3
3.2.1 Mixing Layer Structure	3
3.2.2 Scalar Mixing.	4
3.2.3 Mixing Enhancement	7
3.2.4 Combustion Studies	7
3.3 Future Work	7
4.0 SUPERSONIC FLOW DIAGNOSTICS	9
4.1 Objectives.	9
4.2 Status of the Research.	9
4.2.1 Flow Facility Development	9
4.2.2 Flowfield Code Development.	10
4.2.3 PLIF Imaging of Shock-Induced Ignition	11
4.2.4 PLIF Imaging of Supersonic Jet Mixing and Combustion.	14
4.3 Future Work.	16
5.0 STABILITY ANALYSIS AND NUMERICAL SIMULATIONS	17
5.1 Objective.	17
5.2 Status of the Research	17
5.2.1 Homogeneous Compressible Shear Flow	17
5.2.2 Compressible mixing layer stability analysis	17
5.3 Future Work.	21
6.0 PRESENTATIONS AND PUBLICATIONS	22
6.1 Presentations (2/90 - 2/91).	22
7.0 PERSONNEL	24

1.0 SUMMARY

An experimental and computational investigation of supersonic combustion flows is in progress. The principal objective of the research is to gain a more fundamental understanding of mixing and chemical reaction in supersonic flows. The research effort comprises three inter-related elements: (1) an experimental study of mixing and combustion in a supersonic plane mixing layer; (2) development of laser-induced fluorescence techniques for time-resolved two-dimensional imaging of species concentration, temperature, velocity and pressure; and, (3) numerical simulations of compressible reacting flows. The specific objectives and the status of the research of each of these program elements are summarized in this report.

2.0 INTRODUCTION

Air-breathing propulsion systems offer the potential of higher performance than conventional rocket engines for hypersonic flight. To realize this potential, new combustor design concepts are required. In particular, in order to minimize losses associated with strong shock waves and high combustor inlet temperatures, it is desirable to maintain high flow velocities in the combustion chamber. This design concept leads to a new class of propulsion devices where combustion takes place in supersonic flow.

Combustion in supersonic flow is fundamentally different from combustion in the subsonic flow regime employed in all currently operating aircraft engines. Many of the design approaches developed over the years for subsonic combustors, e.g. ignition and flame stabilization techniques, are not applicable to supersonic combustion devices, and the current understanding of the fundamental aspects of supersonic combustion is inadequate to support the development of these devices.

Recent advances in diagnostic capabilities and significant improvements in our ability to compute such flows offer new opportunities to obtain the needed fundamental understanding of compressible turbulent reacting flows. To achieve this understanding, a closely coordinated experimental and computational program which utilizes state-of-the-art experimental techniques and computational methods is needed. We are engaged in such an effort with support from the Air Force Office of Scientific Research.

The principal objective of the research is to gain a more fundamental understanding of the flow physics and chemistry interactions in compressible turbulent reacting flows. The project comprises three interrelated efforts: (1) an experimental study of mixing and combustion in supersonic flows, (2) development of laser-induced fluorescence techniques for time-resolved multi-dimensional imaging of species concentration, temperature, velocity and pressure in supersonic flows, and (3) simulation and modeling of supersonic flows with mixing and chemical reaction. A close coupling among these efforts is maintained in order to maximize our understanding of supersonic turbulent reacting flows, with emphasis on supersonic combustion. The specific objectives and status of the research of each of the program elements is described below.

3.0 MIXING AND REACTION IN SUPERSONIC FLOW

3.1 Objectives

The objective of this part of the program is the experimental study of mixing and chemical reaction in a compressible mixing layer. Data acquired using conventional and laser-based diagnostics provide important new knowledge about mixing and reaction under compressible conditions.

3.2 Status of the Research

Figure 1 shows a schematic of the flow facility used in the experimental investigation of supersonic mixing and combustion flows. This facility is described in detail in Clemens and Mungal (1990) (see publication list in Section 6.0). Different convective Mach numbers, M_c , are achieved by varying the inlet Mach numbers. Significant experimental findings obtained during the past year are summarized below.

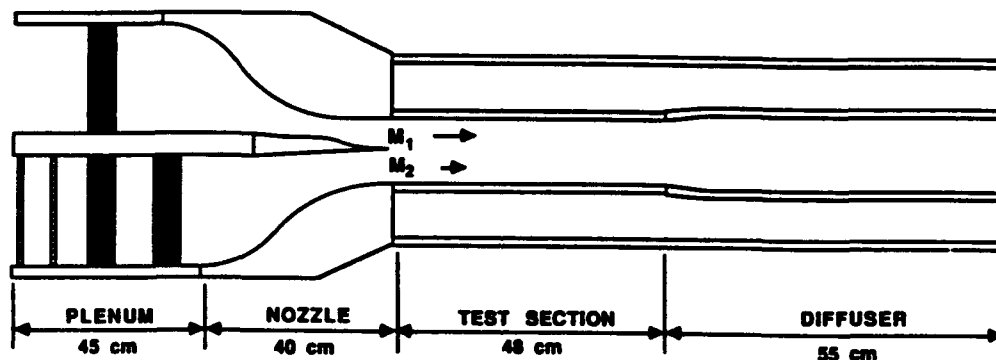


Fig. 1. Schematic diagram of the supersonic flow facility.

3.2.1 Mixing Layer Structure

A more complete series of experiments aimed at investigating the structure of the non-reacting mixing layer at low and high compressibility have been performed. Planar laser Mie scattering has been used to obtain spatially-resolved visualizations of the mixing layer. In this technique, alcohol vapor seeded into the low-speed stream condenses on contact with the cold high-speed stream to form fine alcohol droplets. A laser sheet from a pulsed Nd:Yag laser illuminates the resulting droplet "fog," which effectively marks the mixing region. Images are acquired using a CCD camera, frame grabber and laboratory computer. Full details of the technique can be found in Clemens and Mungal (1991a).

Figure 2 shows representative planar Mie scattering images. Side and plan views of the mixing layer are shown for two different convective Mach numbers, $M_c = 0.28$ and 0.62 , corresponding to low and moderate levels of compressibility. The field of view extends from $x = 15$ to 45 cm downstream of the splitter tip and corresponds roughly to 1000 to 3000 high-speed boundary layer momentum thicknesses downstream. Local Reynolds numbers, based on velocity difference and visual thickness of the layer at the nozzle exit plane, are about 260,000 and 800,000 for the low and high convective Mach numbers, respectively. At low compressibility, the mixing layer generally shows a Brown-Roshko roller-like structure, as can be seen most clearly in the side views. At moderate and high compressibility, the mixing layer is considerably more three dimensional in appearance. These observations are consistent with end views, not shown here. Since the Reynolds numbers of both cases are quite high, we conclude that the observed changes in structure are a compressibility effect and not a Reynolds number effect. Additional details of these experiments are reported in Clemens and Mungal (1990).

3.2.2 Scalar Mixing

Planar laser-induced fluorescence (PLIF) has been used to investigate the scalar mixing field for low and moderate compressibility. In these experiments, NO is seeded at about 1500-3500 ppm into the low-speed stream and acts as a passive scalar. The A-X(0,0) $Q_1(10.5)$ transition of NO is pumped at 226.160 nm with broadband collection of the resulting fluorescence. Due to the quenching conditions and the chosen pump line, the resulting fluorescence signal can be shown to be proportional to the NO mole fraction.

Two typical results are shown in Fig. 3. The small inset photograph shows the NO mole fraction across a small region of the flow extending from $x = 28$ to 33 cm. In this photograph, white represents low-speed fluid, black represents high-speed fluid, with intermediate grey levels representing mixed fluid. To better reveal the scalar concentration field, the larger photograph presents the same information, where intensity has been converted to height. This perspective view is equivalent to viewing the scalar field from the high-speed stream to the low-speed stream. The low compressibility case shows NO mole fractions which tend to be uniform in the cross-stream direction and ramped in the streamwise direction. The moderate compressibility case also shows streamwise ramps, but two levels of NO mole fraction are observed in the cross-stream direction. Work is continuing on the interpretation of the PLIF images and on the calculation of statistical measures such as the probability density function of NO mole fraction. These results will be presented in Clemens et al. (1991).

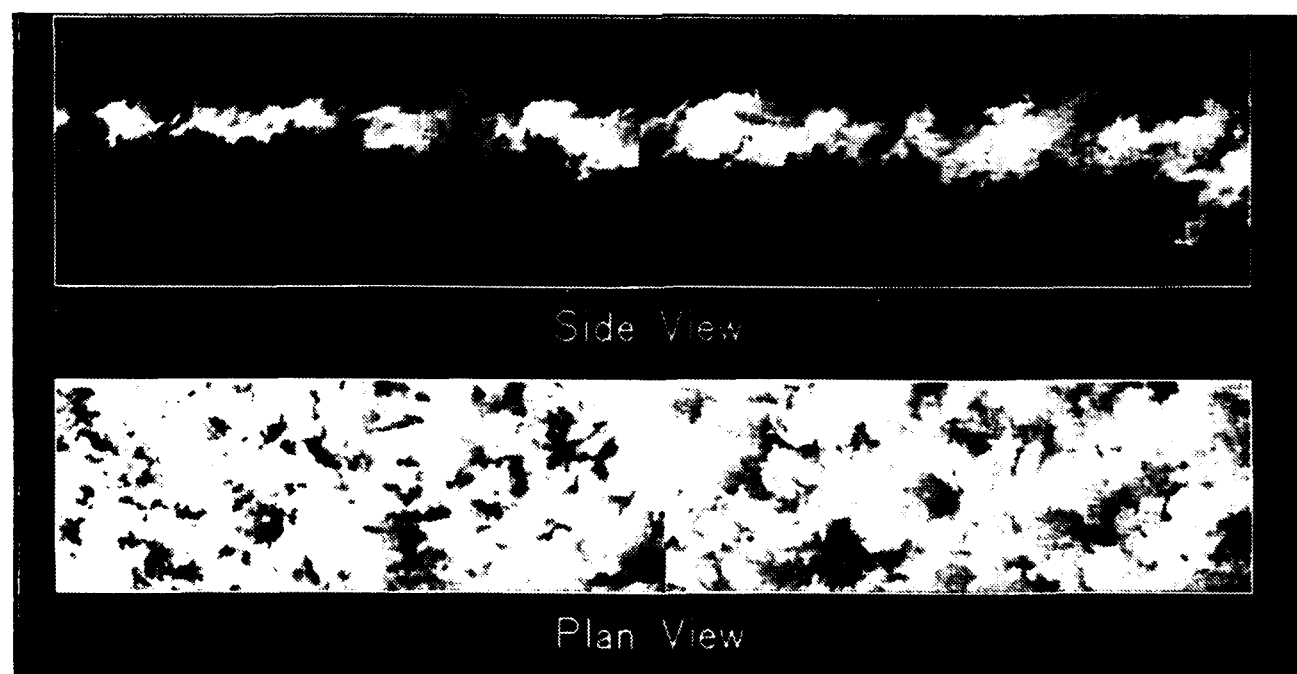
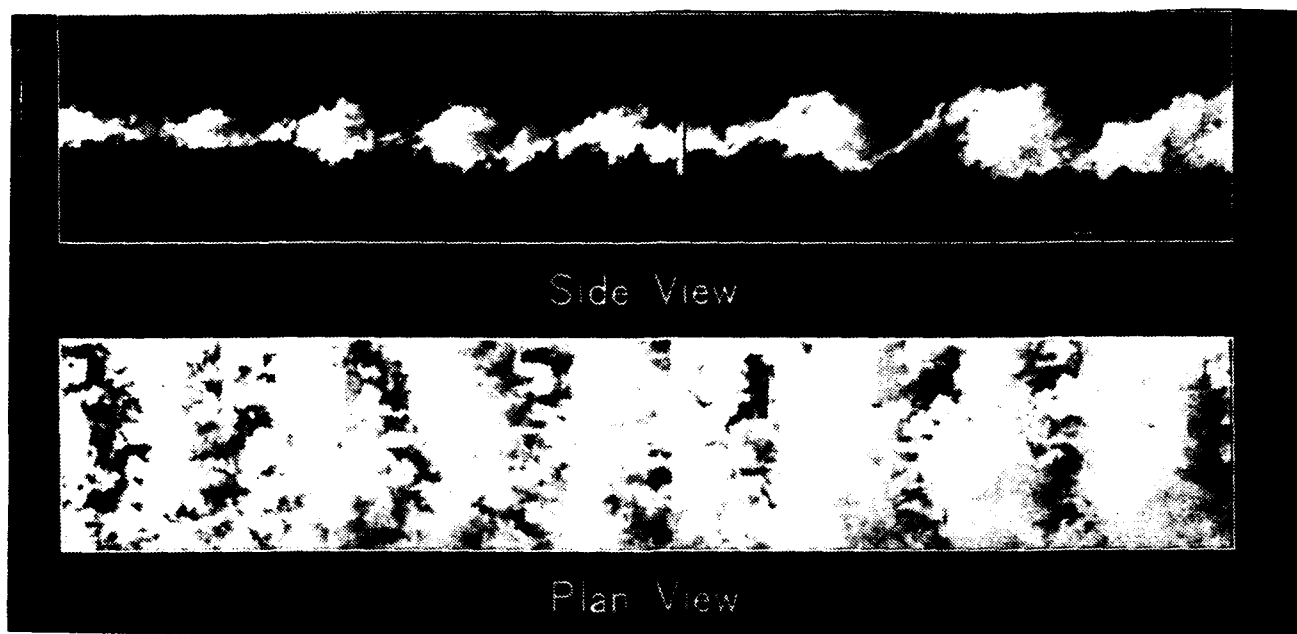


Fig. 2. Planar laser Mie scattering visualizations of the mixing layer. Top: $M_c = 0.28$; Bottom: $M_c = 0.62$.

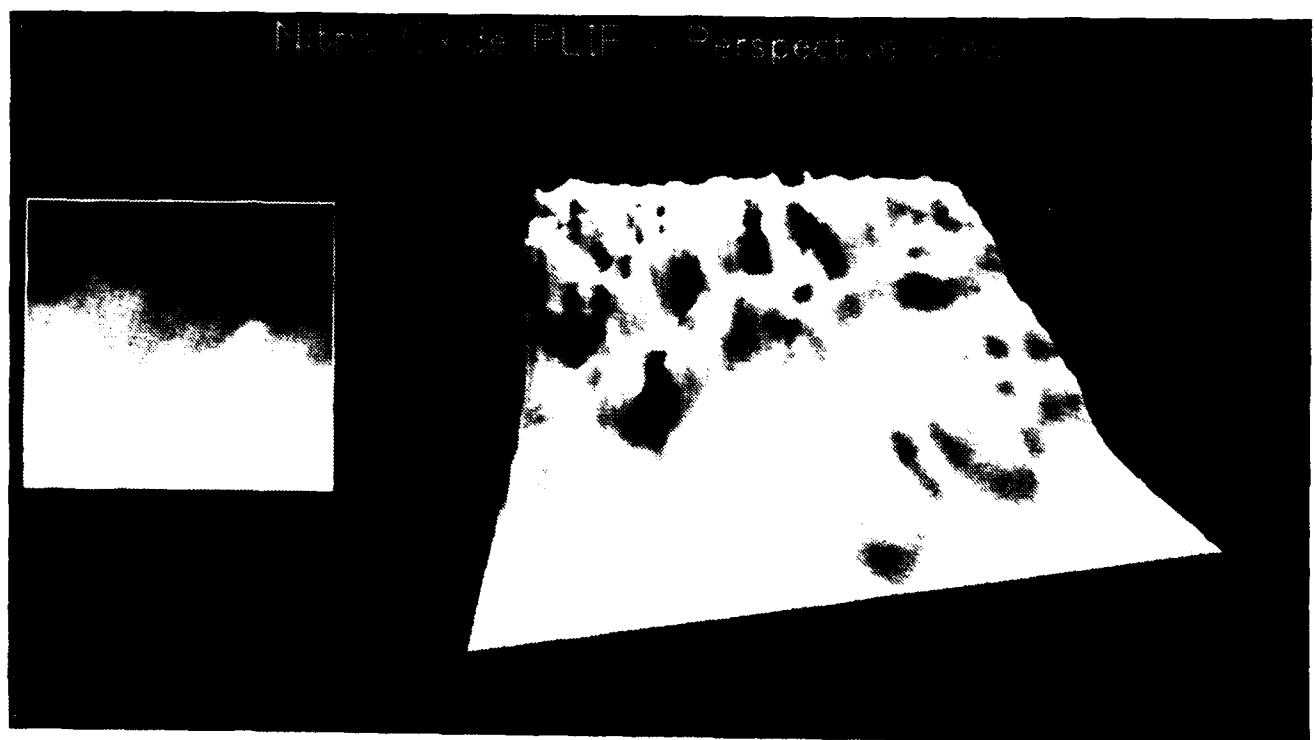
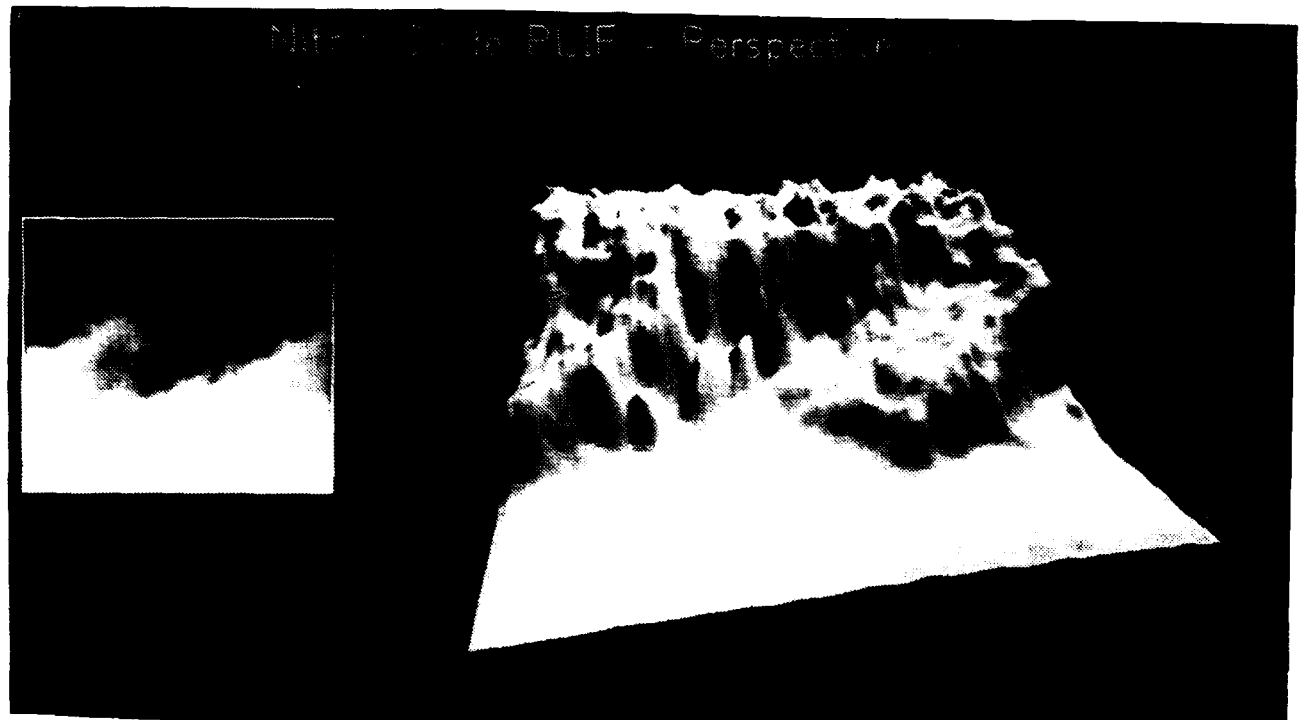


Fig. 3. PLIF images of NO mole fraction in the mixing layer. Top: $M_c = 0.28$; Bottom: $M_c = 0.62$.

3.2.3 Mixing Enhancement

During the course of our non-reacting flow studies, we found that side-wall disturbances, rather than spanwise disturbances, have the potential to change the mixing layer structure in a dramatic way. Figure 4(a) shows how a side-wall disturbance generator located inside of the supersonic nozzle upstream of the splitter tip can launch a shock wave which interacts with the splitter tip and disrupts the layer. Figure 4(b) shows a time-averaged end view of the mixing layer with a single side-wall disturbance generator. The strong distortion of the layer is evident leading to increased mixing volume. Clemens and Mungal (1991b) provide additional details about this approach for mixing enhancement. Given that a wave system is used to produce the layer perturbations, we conclude that the response of the layer seen here has no analog in subsonic flow.

3.2.4 Combustion Studies

We recently have configured the supersonic flow facility for combustion tests. Specifically, the vitiation air heater has been operated over a broad range of temperatures. Stagnation temperatures up to 1800 K, needed to produce ignition in the mixing layer, have been achieved. A splitter tip has been designed and fabricated for the combustion tests to provide convective Mach numbers which overlap those used in the non-reacting flow experiments. A make-up oxygen flow system has been designed for the high-speed vitiated air stream and a hydrogen flow system for the low-speed stream has been installed. Initial combustion tests will be conducted to establish the ignition envelope for the facility.

3.3 Future Work

During the next year, we plan to continue the work discussed above with emphasis on the combustion and mixing enhancement aspects. This work includes:

- Complete statistical analysis of PLIF data for the non-reacting mixing layer.
- Investigation of the ignition process for hydrogen-vitiated air streams for compressible conditions.
- Examination of the structure of the compressible reacting mixing layer for variable heat release.
- Exploration of the effects of Damköhler number for compressible conditions.

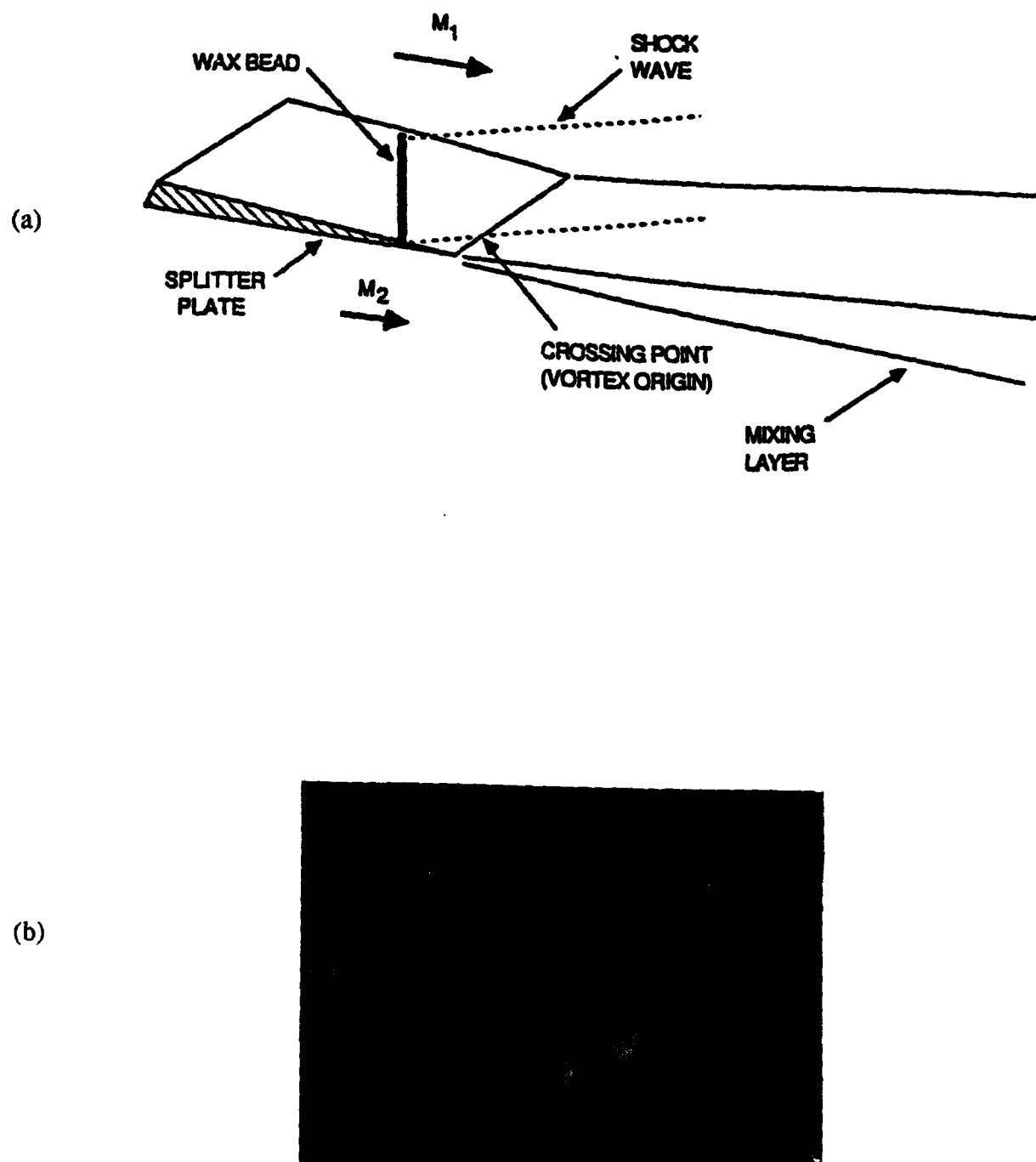


Fig. 4. Effects of a single side-wall disturbance generator on the mixing layer. (a) schematic diagram; (b) resulting flowfield perturbation when viewed upstream at $x = 25$ cm. $M_c = 0.28$.

4.0 SUPERSONIC FLOW DIAGNOSTICS

4.1 Objectives

This element of our research program is aimed at developing flowfield imaging diagnostics based on Planar Laser-Induced Fluorescence (PLIF). Flow parameters of interest include species concentrations (or mole fractions), temperature, velocity and pressure. Particular emphasis is placed on imaging nitric oxide (NO), molecular oxygen (O_2) and hydroxyl radicals (OH), since these species are naturally present in most supersonic propulsion flows of interest.

4.2 Status of the Research

Work over this reporting period has been in four areas: (1) flow facility development; (2) code development for method-of-characteristics solutions of nonequilibrium supersonic free jets; (3) PLIF imaging experiments of shock-induced ignition phenomena; and (4) PLIF imaging of mixing and combustion of transverse jets in shock-generated supersonic flow.

4.2.1 Flow Facility Development

There have been three flow facility projects, all associated with our shock tube. The primary project, now nearing completion, has involved design and assembly of a shock tunnel extension to the shock tube. This shock tunnel comprises a dump tank, supersonic free jet test section, and hardware to couple the test section to the existing shock tube. In these experiments, reflected shock waves will be used to generate controlled, high temperature and pressure stagnation conditions, and the gas will flow into the dump tank through a converging nozzle. The result will be an underexpanded supersonic free jet with a wide range of temperature, pressure and velocity along the jet centerline. This flowfield is ideal for developing and testing new diagnostics since it: (1) is an economical design (no contoured diverging nozzle needed); (2) provides an extremely wide range of flow conditions in a single flow; and (3) gives good optical access. The flowfield conditions can also be chosen to provide varying degrees of nonequilibrium (e.g., vibrational nonequilibrium with separate vibrational and translational/rotational temperatures); this enables important tests of the suitability of various diagnostic strategies to deal with nonequilibrium supersonic flows. We expect to begin check-out tests of the shock tunnel within the next three months.

A second facility project involved modifying the planar end wall of the shock tube to include a shallow v-groove. The objective was to provide slightly nonuniform shock wave reflection, leading to localized ignition of shock-heated fuel-oxidizer mixtures. This work was completed and published during the past year (see publication list in Sec. 6.0).

Finally, we modified the side wall of the shock tube to incorporate a pulsed valve assembly. The objective was to provide a facility for studying the mixing and combustion of a transverse jet in a supersonic cross-flow. A first-generation jet injection system was built and tested, leading to research on PLIF imaging of mixing and burning jets presented and published at the recent 23rd International Combustion Symposium (see publication listed in Sec. 6.0).

4.2.2 Flowfield Code Development

During the past two years we have been working to assemble a computer code to describe nonequilibrium supersonic free jets. This code will be needed to evaluate the PLIF imaging data acquired in our shock tunnel. At the present time, the code is able to handle three critical flowfield cases: (1) constant gamma (ratio of specific heats); (2) vibrationally equilibrated flow (infinite relaxation rate); and (3) finite relaxation rate. In each case, the code calculates the entire flow between the nozzle exit (sonic condition) and the Mach disc. An example result showing the variation of temperature along the jet centerline is shown in Fig. 5. In this case, the flow is 100% O_2 , but several different mixtures involving various proportions of $NO/O_2/N_2/Ar$ are of interest and will be studied. Note that results are provided for both the vibrational and translational/rotational temperatures and for a range of vibrational relaxation rates (frozen flow, finite rate relaxation, and equilibrium flow).

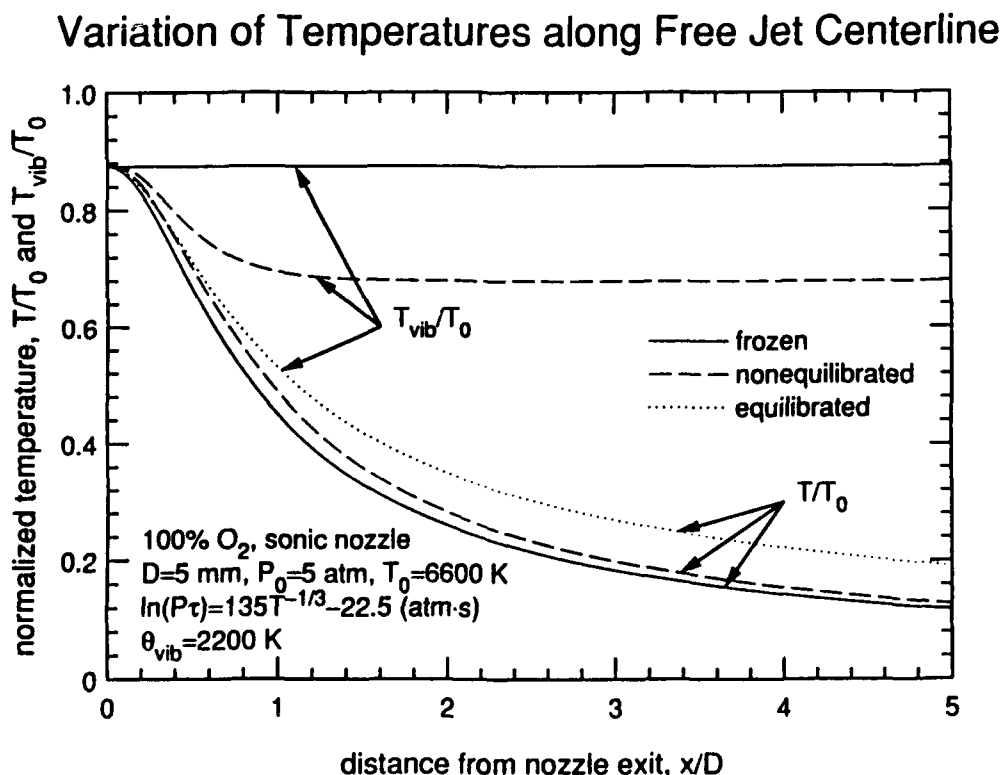


Fig. 5. Method-of-characteristics solutions for temperature on centerline of an underexpanded free jet with vibrational relaxation.

In conducting PLIF imaging of these flows, we hope to establish strategies for monitoring both the vibrational and translational/rotational temperatures, as well as finding schemes for imaging velocity and pressure.

In the future, we will explore extension of the method-of-characteristics code to include chemical nonequilibrium.

4.2.3 PLIF Imaging of Shock-Induced Ignition

In this program we have been concerned with developing PLIF imaging strategies suited for monitoring ignition phenomena in H_2-O_2 mixtures at elevated temperatures. The approach we have taken is to monitor OH production in the region behind a reflected shock wave. The shock tube end wall was modified to include a shallow groove, so that local nonuniformities in post-shock temperature are created after shock reflection. The influence of the resulting temperature variations is to cause localized ignition, which then spreads as a moving flame front, since the ignition reactions are highly temperature sensitive. This flowfield provide an interesting and relevant testing ground for the development of PLIF imaging in reactive flows. Problems encountered and solved include: optimized selection of the laser source, selection of the appropriate OH transition, and several difficulties associated with synchronization of the shock tube, fuel-oxidizer ignition, laser pulse, and intensified camera gating.

Sketches of the experimental arrangement and imaging geometry typically employed are shown in Figs. 6 and 7. Sample results for the case of strong ignition (i.e., relatively high temperature flowfields) are shown in Fig. 8. Results were obtained near both the weak- and strong-ignition limits, with the former showing much greater three-dimensionality, as expected. The results for strong ignition exhibit two-dimensional behavior, as is apparent in Fig. 8. In all these data sets, the images essentially represent the instantaneous mole fraction of OH as produced by the ignition occurring behind the reflected shock wave. Note the emergence of a jet of hot fluid from the groove, leading to a triangle-shaped burned region bounded by nearly straight flame fronts. The forward flame front is co-planar with the reflected shock wave which has moved out of the field of view. Combustion also is apparent in the remainder of the reflected shock zone, but the lower temperatures lead to a slight time delay in this process. Eventually, the combustion fronts merge into a single planar front which moves away from the end wall at a constant flame speed.

Details of this work appear in publications cited in Sec. 6.0. It should also be noted that we benefited greatly from informative discussions held with Prof. Oppenheim of UC Berkeley, an expert in the field of reactive gasdynamics who has published several papers on shock-induced ignition. His work, however, was limited to conventional flowfield visualization schemes, such as schlieren, based on line-of-sight concepts. Comparisons of our data with his earlier results provided convincing proof of the merit of PLIF as a spatially resolved, species-specific diagnostic.

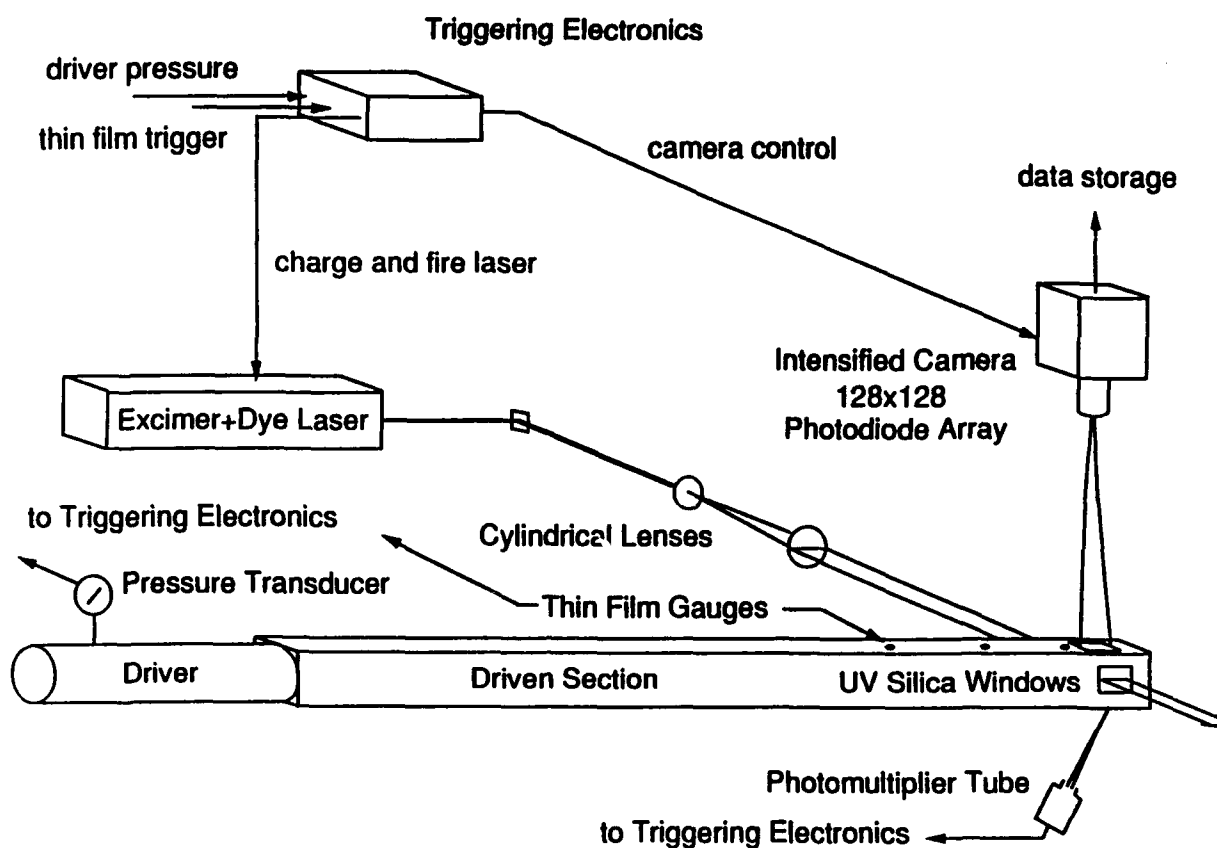


Fig. 6. Schematic of shock tube facility for PLIF imaging.

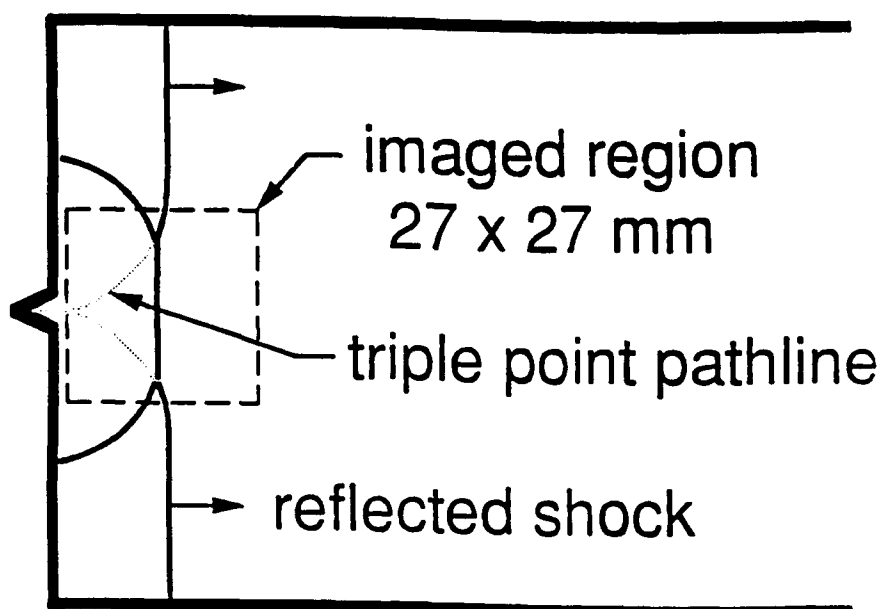


Fig. 7. Schematic of imaging geometry for the endwall with the vertical V-shaped groove down the center. The reflected shock structure a short time after reflection is sketched qualitatively.

Fig. 8a

Fig. 8b

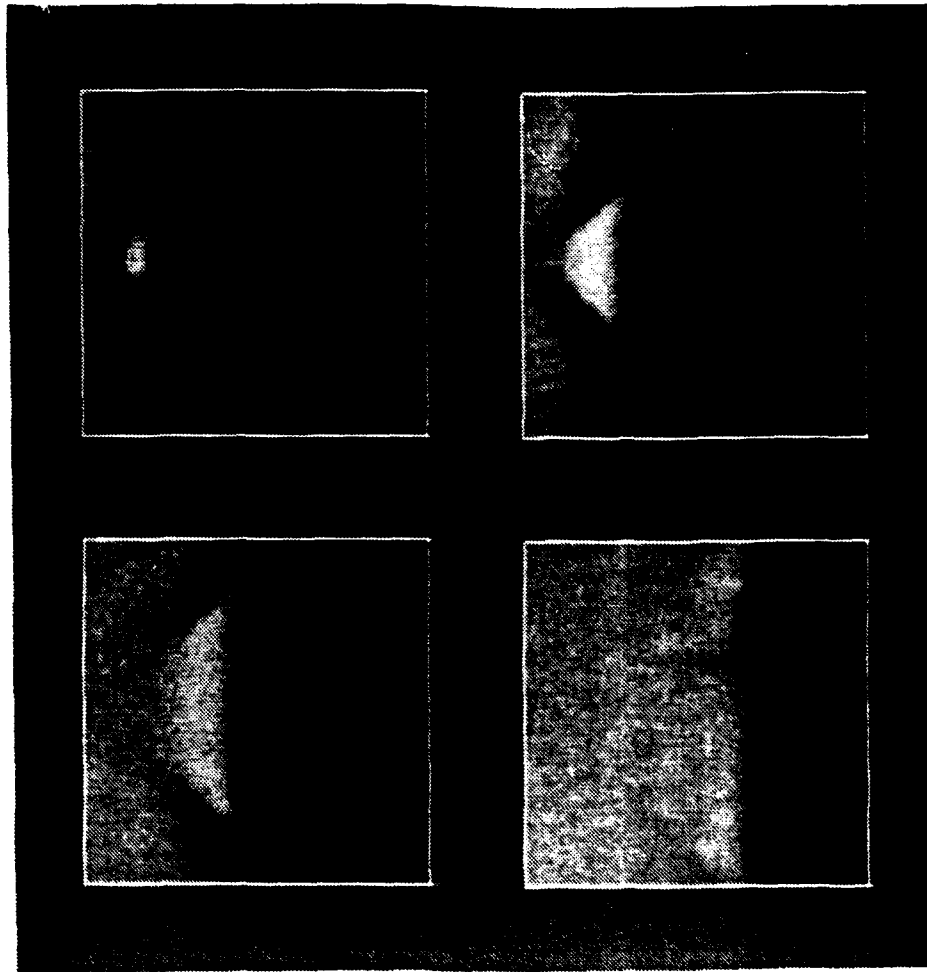


Fig. 8c

Fig. 8d

Fig. 8. Sequence of four PLIF images of OH acquired in the strong ignition limit behind a shock reflected off the V-groove endwall. The image in (a) was acquired $\sim 35 \mu\text{sec}$ after shock reflection. Images (b), (c) and (d) were acquired in separate experiments at delays of 10, 25 and 45 μsec with respect to (a). Neglecting the effect of the nonplanar endwall, the conditions behind the reflected shock were 1440 K and 1.9 atm and the reflected shock speed was 0.45 mm/ μsec .

4.2.4 PLIF Imaging of Supersonic Jet Mixing and Combustion

Our most recent activity has been to investigate PLIF approaches to the imaging of transverse jets in supersonic cross-flow. In particular, the objective is to develop methods for imaging critical aspects of the mixing and combustion which occur in such jets; this would include measurements of jet mixture fraction, flame front location, combustion products, temperature, velocity and pressure. This gasdynamics problem is relevant to current research and development of scramjet engines. Because past measurements in such flows were based exclusively on conventional instrumentation such as pressure gauges, interferometry, schlieren, radiative emission, etc., there is a high potential payoff for the successful development of nonintrusive imaging schemes which can yield some of the properties noted above.

In order to provide a meaningful environment which simulates critical aspects of the jet mixing and combustion problem, we have modified our shock tube to allow injection of gases into the supersonic flow behind an incident shock wave. At present we employ a pulsed valve, with a 2 mm round orifice, which was custom-built to allow rapid opening. We have conducted tests with nonreacting and reacting jets. In the nonreacting case, a jet of 5% NO in N₂ was injected into a freestream of 21% N₂ in argon, while in the reacting flow study the jet was pure H₂ and the freestream was 21% O₂ in argon. In both cases, the jet stagnation conditions were nominally 300K and 3.4 atm, the freestream Mach number was 1.4 and the freestream static temperature and pressure were 2100K and 0.39 atm, respectively. Imaging measurements of NO, in the nonreacting case, essentially represent the jet mixture mole fraction, the quantity of primary interest in characterizing the mixing of the jet fluid. In the case of the reacting jet, we imaged OH, which essentially is an indicator of the flame front.

A sketch of the flowfield is provided in Fig. 9. Sample results (centerline images along the shock tube axis) for the nonreacting case (both single-shot and time-averaged) are shown in Fig. 10. Note particularly the presence of large-scale structures in the instantaneous image; these features of course disappear in the time-averaged data. We believe that these structures are likely to play a key role in the mixing of high-speed jets, and yet their presence is not accounted for in current models (usually time-averaged) of jet mixing. Finally, a comparison of end-view images of the nonreacting and reacting cases is shown in Fig. 11. The OH image shows that the flame front is nearly round in this view, surrounding the unburned fuel jet. The nonreacting case, by contrast, has no hollow core since the quantity being monitored is representative of the jet fluid. Also, note the evidence at this axial location of interaction between the jet fluid and the wall boundary layer.

PULSED JET/FLOWFIELD CHARACTERISTICS

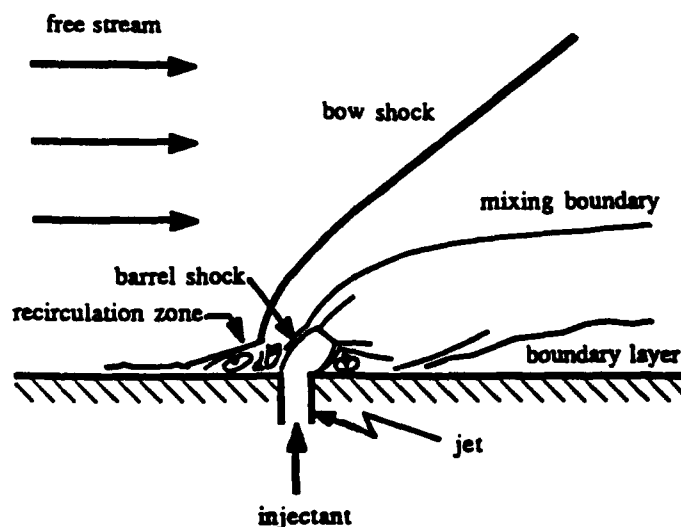


Fig. 9. Schematic of the flowfield, illustrating the characteristic flow features.

Fig. 10a

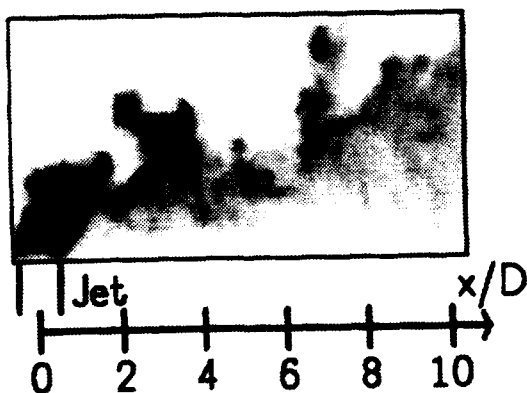


Fig. 10b

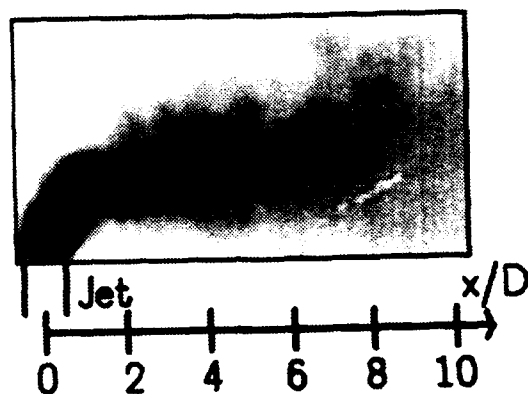


Fig. 10. PLIF images of NO acquired in the side-view geometry displayed in Fig. 9. (a) Single-shot PLIF of NO. (b) 12-frame average PLIF image of NO. Signal is presented in a continuous gray scale, where white indicates low signal and black indicates high signal. The imaged area is 22×22 mm trimmed down to 11×22 mm, and extends from $x/D = -1$ to $x/D = 10$ in the axial direction.

Fig. 11a

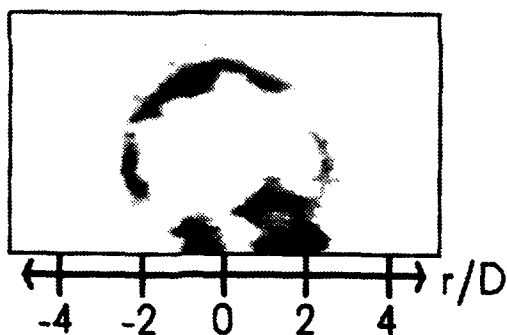


Fig. 11b

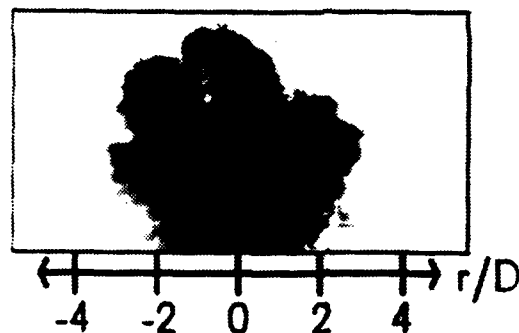


Fig. 11. End-view PLIF images of NO and OH at an axial location $x/D = 15$. (a) Single-shot PLIF image of OH. (b) Single-shot image of NO. The imaged region shown is 11×22 mm.

We believe that these images represent the first single-shot PLIF data for this important flow. The shock tube appears to be a convenient, economical vehicle for generating these flows, and we have solved the various difficulties encountered in synchronizing the shock wave motion, jet valve opening, laser firing, intensifier gating, and image recording on the photodiode array. For further details of this work, the reader is directed to the publications cited in Sec. 6.0.

4.3 Future Work

During the next year of this program we plan to continue some of the activities described above and initiate related work. This work includes:

- Complete assembly and characterization of the shock tunnel.
- Perform PLIF imaging in supersonic free jet to establish strategies for sensing critical flow parameters in vibrational and chemical nonequilibrium flows.
- Continue research on the development of PLIF imaging techniques to study transverse nonreacting and reacting jets in supersonic cross-flow.

5.0 STABILITY ANALYSIS AND NUMERICAL SIMULATIONS

5.1 Objective

The objective of this portion of the program is to use stability analysis and numerical solutions of the governing equations to provide insight into the important physics controlling mixing and reaction in high-speed flows. Two basic flows are being considered - (a) homogeneous compressible shear flow and (b) the compressible mixing layer.

5.2 Status of the Research

5.2.1 Homogeneous Compressible Shear Flow

The purpose of our work on homogeneous compressible shear flows is to develop and understanding of the small-scale structure and microscopic mixing in compressible shear flows. A comprehensive report on the homogeneous shear flow work is now in press (Blaisdeli et al., 1991). This study revealed several important features of the fine-scale structure in compressible shear flows. Of particular importance to turbulence modeling is the confirmation of the importance of dilatation dissipation associated with sparsely-distributed eddy shocklets. The ratio of the dilatation dissipation to the total dissipation was shown to approach a constant independent of the initial conditions, and there is evidence that the rms Mach number of the fluctuations approaches an asymptotic value of the order of 0.7.

5.2.2 Compressible mixing layer: stability analysis

The purpose of this work is to develop understanding of the large-scale structure and macroscopic mixing in compressible mixing layers. Linearized stability analysis and accurate direct numerical simulations are the tools employed.

We recently have carried out detailed studies of the stability of a compressible mixing layer with heat release. There are three important results from this work:

- (a). Without heat release, the dominant instability modes are associated with concentrated vorticity in the center of the mixing layer. The dominant mode is two-dimensional at low Mach numbers, but becomes three-dimensional above convective Mach numbers of about 0.7. This result suggests that the classical two-dimensional vortex merging flow observed in low-speed mixing layers is replaced in supersonic flow by a much more complex three-dimensional vortical flow. This observation has indeed been confirmed by both numerical simulations and our experiments.

- (b). As a result of the change in the mean vorticity and density profiles with the heat release at a flame front in the mixing layer, there are two dominant instability modes, one associated with strong vorticity in the fast stream and the other with strong vorticity in the slow stream. These modes, referred to as the outer modes, are also present without heat release at sufficiently high convective Mach numbers. Surprisingly, with heat release, the dominant modes are two-dimensional to much higher Mach numbers than without heat release. However, with two competing vortical modes, the resulting flow can be expected to be much more complex than low-speed flows, as will be shown below.
- (c). With heat release, the behavior of the instability modes is not well correlated with the convective Mach number that is used to correlate compressible non-reacting mixing layers. This is because the standard convective Mach number is based on an analysis that assumes isentropic flow in each stream to a stagnation point in the moving reference frame. We have introduced a new parameter, the *flame convective Mach number*, which correlates the instability behavior extremely well. Figure 12 shows the amplification rate for a typical heat release case plotted against the standard convective Mach number. The lines represent the case without heat release, and the symbols the case with heat release. Comparing Figure 12 with Figure 13, where the same data are plotted versus flame convective Mach number, we see that the two cases are nearly identical in terms of this parameter. This result suggests that flame convective Mach number will be the preferred parameter for correlation of laboratory reacting flow data.

Direct numerical simulations confirm the trends suggested by the stability analysis. These simulations show that the fast and slow outer modes slide on each other without interacting. As a consequence, no flame surface is generated and mixing of fuel and oxidizer by large-scale structures does not occur. The probability density function of the mixture fractions exhibits two bumps (Fig. 14). In this figure, it is seen that fuel is mixed with product by the fast outer mode and oxidizer is mixed with product by the slow outer mode. Although subharmonics in the initial field were included to induce vortex pairing, no pairing occurs in the outer modes. Instead, there is a slow accretion of one mode into the other.

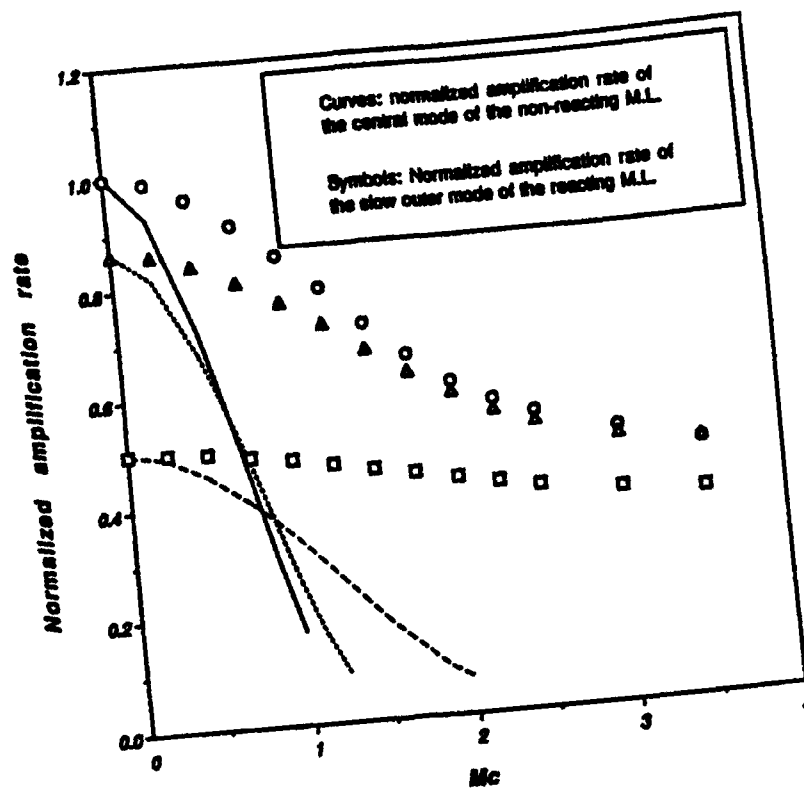


Fig. 12. Amplification rate versus the standard convective Mach number for mixing layers with heat release.

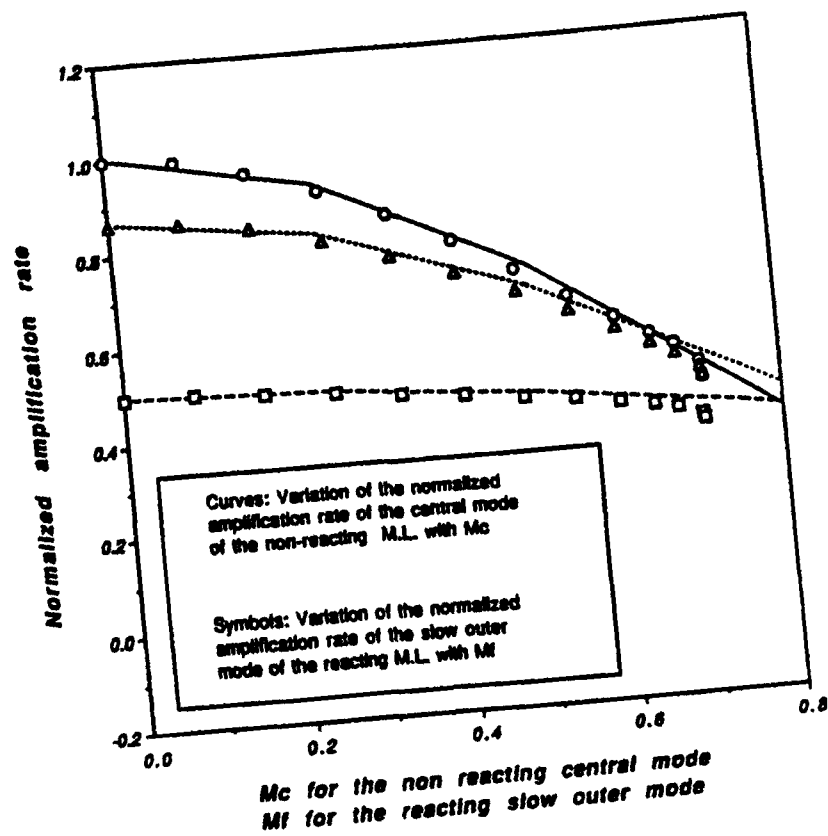


Fig. 13. Amplification rate versus the flame convective Mach number for mixing layers with heat release.

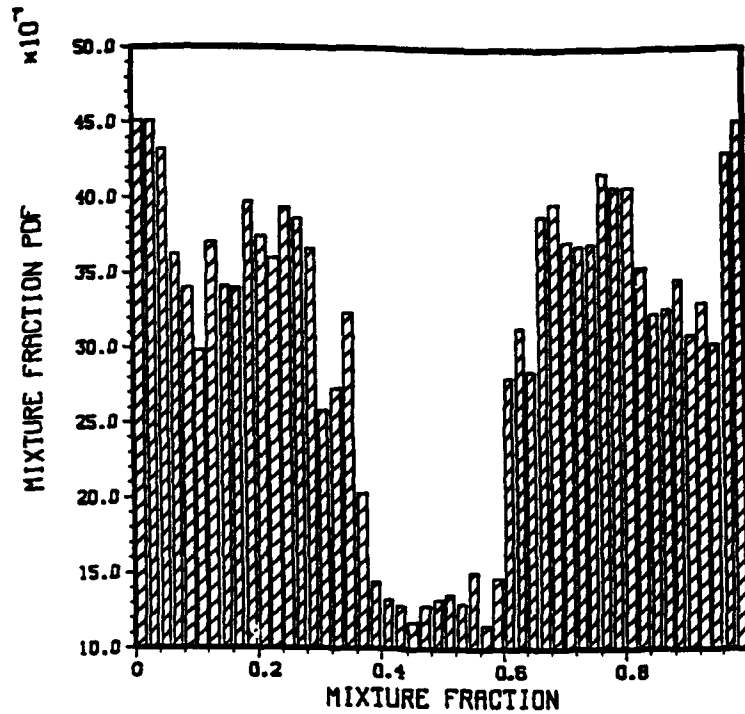


Fig. 14. Typical mixture fraction PDF of a compressible reacting mixing layer ($M_c = 0.8$).

Results from the flow experiments, described in Section 3.0, appear to confirm the existence of the outer modes which occur even without heat release at sufficiently high convective Mach numbers. These experiments displayed two distinct ramps of mixture fraction on the PLIF images of NO at $M_c = 0.62$, similar to the two ramps observed in the simulations whenever the outer modes are present (Fig. 15). The existence of the two ramps implies that mixing models based on large-scale structure engulfment from both sides of the mixing layer may not be appropriate in compressible reacting mixing layers.

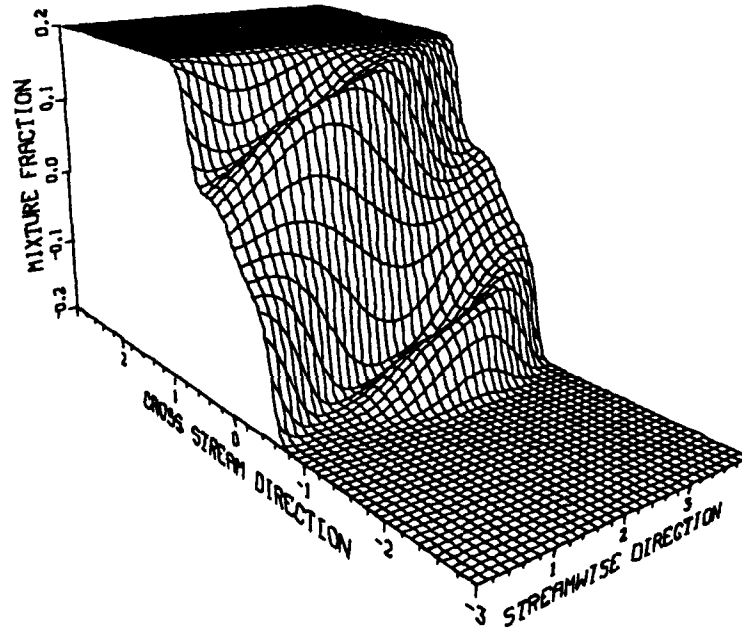


Fig. 15. Typical spatial distribution of the mixture fraction for supersonic reacting shear layers.

5.3 Future Work

During the next year, we plan to work in the following areas:

- Slow chemistry effects and the mechanism for mixing layer growth.

We will assess the effects of slow chemistry on the mixing process. We also will investigate the overall growth mechanism of the reacting compressible mixing layer.

- Three dimensionality issue.

We will address the question: Does heat release cause the large-scale structures of the reacting shear layer to remain two-dimensional at high Mach numbers, as predicted by the linear stability analysis? This issue is important in terms of its effects on entrainment and subsequent mixing process.

- Ignition delay and spatial simulations.

The existence of a significant ignition delay for hydrogen-air combustion and the short residence time associated with supersonic flows, indicate that mixing might partially occur before reaction. The combustion regime would then differ from the diffusion flame regime between two zones of mixing assumed in our simulations to date.

6.0 PRESENTATIONS AND PUBLICATIONS

6.1 Presentations (2/90 - 2/91)

1. G. A. Blaisdell, N. Mansour and W. C. Reynolds (1990), "Numerical Simulations of Compressible Homogeneous Turbulence," Report TF-50, Mechanical Engineering Report, Stanford University.
2. O. Planche and W. C. Reynolds (1990), "Compressibility Effects on the Supersonic Reacting Mixing Layer," AIAA-90-0739, AIAA Aerospace Sciences Meeting.
3. N. T. Clemens and M. G. Mungal (1990), "Two- and Three-Dimensional Effects in the Supersonic Mixing Layer", AIAA-90-1978, AIAA Aerospace Sciences Meeting, also to appear AIAA J.
4. R. K. Hanson (1990), "Planar Fluorescence Imaging: Concepts and Applications," invited presentation at NATO Advanced Study Institute, Algarve, Portugal.
5. B. K. McMillin, M. P. Lee, P. H. Paul and R. K. Hanson (1990), "Planar Laser-Induced Fluorescence Imaging of Shock-Induced Ignition," *Twenty-Third Symposium (International) on Combustion*, The Combustion Institute, in press; presented at Twenty-Third Symposium (International) on Combustion, Orleans, France.
6. P. H. Paul, M. P. Lee, B. K. McMillin, J. M. Seitzman and R. K. Hanson (1990), "Application of Planar Laser-Induced Fluorescence Imaging Diagnostics to Supersonic Reacting Flow," paper 90-1844 at 28th AIAA/SAE/ASME/ASEE Joint Propulsion Conf., Orlando, FL.
7. R. K. Hanson, A. Y. Chang, M. D. DiRosa, L. C. Philippe, B. K. McMillin and M. P. Lee (1990), "Laser-Based Diagnostics for Propulsion and Hypersonics Testing," paper AIAA-90-1383 presented at AIAA 16th Aerodynamic Ground Testing Conf., Seattle WA.
8. B. K. McMillin, P. H. Paul and R. K. Hanson (1990), "Planar Laser-Induced Fluorescence Imaging of Nitric Oxide in Shock Tube Flows with Vibrational Nonequilibrium," AIAA J., in press; also paper AIAA-90-1519 at AIAA 21st Fluid Dynamics, Plasmadynamics and Lasers Conf., Seattle WA.
9. J. L. Palmer, B. K. McMillin and R. K. Hanson (1991), "Planar Laser-Induced Fluorescence Imaging of Underexpanded Free Jet Flow in a Shock Tunnel Facility," to be presented at AIAA 22nd Fluid Dynamics, Plasma Dynamics and Lasers Conference, Honolulu, Hawaii.
10. M. P. Lee, B. K. McMillin, J. L. Palmer and R. K. Hanson (1991), "Two-Dimensional Imaging of Mixing and Combustion of Transverse Jets in Shock Tube Flows," submitted to J. Prop. and Power.

11. N. T. Clemens and M. G. Mungal (1991a), "A Planar Mie Scattering Technique for Visualizing Supersonic Mixing Flows", to appear Expts. Fluids.
12. N. T. Clemens and M. G. Mungal (1991b), "Effects of Side-Wall Disturbances on the Supersonic Mixing Layer", to appear J. Prop. Power.
13. N. T. Clemens, P. H. Paul, M. G. Mungal, and R. K. Hanson (1991), "Scalar Mixing in the Supersonic Shear Layer", AIAA-91-1720, to be presented at the AIAA 21st Fluid Dynamics, Plasma Dynamics and Lasers Conference).

7.0 PERSONNEL

Craig T. Bowman	Professor, Mechanical Engineering
Ronald K. Hanson	Professor, Mechanical Engineering
Mark Godfrey Mungal	Assistant Professor, Mechanical Engineering
William C. Reynolds	Professor, Mechanical Engineering
Phillip H. Paul	Senior Research Associate, Mechanical Engineering
Gregory A. Blaisdell	Graduate Research Assistant, Mechanical Engineering
Noel T. Clemens	Graduate Research Assistant, Mechanical Engineering
Tobin Island	Graduate Research Assistant, Mechanical Engineering
Michael P. Lee	Graduate Research Assistant, Mechanical Engineering
Brian McMillin	Graduate Research Assistant, Mechanical Engineering
Michael F. Miller	Graduate Research Assistant, Mechanical Engineering
Olivier Planche	Graduate Research Assistant, Mechanical Engineering
Jennifer Palmer	Graduate Research Assistant, Mechanical Engineering